_____

Enhancing Sustainability in Smart Cities: IoT-Enabled with Fog and Haze Mitigation Using EDN-GTM Technology

Sahil Godara
Research Scholar, Department of Computer Science and Applications,
Baba Mastnath University, Rohtak, Haryana, India (sahilgodara093@gmail.com)

Dr. Vinod Kumar Srivastava
Professor, Department of Computer Science and Applications,
Baba Mastnath University, Rohtak, Haryana, India

Abstract- the growing reliance on Information and Communication Technologies (ICT) has prompted a shift towards smart city concepts, especially as over 70 per cent of the global population is expected to reside in urban areas by 2050. The smart city paradigm addresses the challenges of managing critical infrastructure by integrating intelligent ICT solutions across various sectors such as the economy, mobility, environment, people, living spaces, and governance. Central to this vision is the Internet of Things (IoT) role, acting as a pivotal network connecting devices and enabling seamless interactions in urban settings. Efficient energy usage is a key aspect of IoT-enabled smart cities, given the increasing demand for power with population growth. Lighting, a fundamental need, consumes a significant portion of energy, and an SLS becomes crucial for effective energy management in a smart city leveraging IoT technologies. The proposed system aims to enhance image quality and address fog-related challenges in Smart City applications by integrating IoT-based technology. In urban environments, foggy conditions can significantly impact visibility, affecting surveillance and monitoring systems. The system employs a comprehensive approach, utilising sensor data, image processing techniques, and deep learning models for efficient fog detection and removal. Key objectives include fog removal and image quality enhancement, focusing on adaptability to varying environmental conditions. The system dynamically adjusts fog removal processes based on real-time fog density information collected from cloud-based sensors. The dataset for training and evaluation is obtained from Kaggle, comprising fully foggy images. Pre-processing involves grey conversion and wavelet transform filters, simplifying image representation and extracting relevant features for subsequent stages. Segmentation with a region of interest (ROI) approach optimises processing efficiency by focusing on information-rich areas. Enhanced Dehazing Network (EDN) and Guided Transmission Map (GTM) models are separately implemented for haze removal and transmission map refinement. A hybrid approach combines the strengths of both models, aiming for superior fog removal and image quality improvement. Performance is assessed using metrics like PSNR, SSIM, TMQI, and FSIMc, providing a comprehensive evaluation. The proposed system, leveraging deep learning, adaptive processing, and IoT integration, offers an effective solution for mitigating the impact of foggy conditions in Smart City scenarios.

Keywords: Enhanced Dehazing Network, Guided Transmission Map, Internet of Things

INTRODUCTION

Our reliance on ICT has surged, and with over 70 percent of the global population predicted to reside in urban areas by 2050, managing critical infrastructure becomes imperative. The smart city concept tackles these challenges comprehensively by incorporating intelligent ICT solutions. Envisioned as the future of urban living, a smart city integrates advanced technologies across sectors like the economy, mobility, environment, people, living spaces, and governance. Additionally, the IoT plays a pivotal role in this vision, acting as a network that connects devices and facilitates seamless interaction in urban settings, promoting efficient resource management across various applications[1-2].

An important part of an IoT-enabled neat city is ensuring energy is used efficiently. This is because as the population grows, so does the need for power, but there are only so many resources. Lighting is a basic need for power in both public and private homes. These days, outdoor lighting uses about 10% of all the energy sent out [3]. Much electricity is

_____

also wasted because of the lights in hospitals, businesses and big apartment buildings. Without question, an SLS is needed to manage and control lighting systems well in a smart city that uses many IoT technologies.

An automatic and smart lighting control system called a Smart Lighting System (SLS) is run by different IoT communication protocols, devices, and their sensors in one place or across many places. An SLS [4]is based on the idea of an efficient lighting system and controlling how much energy homes, workplaces, and streets use. An SLS connected to the IoT can help cut down on wasted power in a smart city. There are three main parts to the design of IoT-enabled SLS: the perception or sensor layer, the communication layer, and the organization layer [5-7]. Sensors built into the light nodes allow mechanical control based on the amount of light (using a light sensor) or the attendance of a person (using a motion sensor). With IoT connection protocol[8], these light nodes can talk to each other and send sensor data. For power management to work well there needs to be a system that can look at the given data and make decisions independently. We here are writing about IoT-enabled Smart Lighting Communication Protocols for smart cities that can be used to control power more effectively. [9-10]

MATERIAL AND METHOD

IoT-based fog detection systems enhance visibility and safety in smart city environments, especially when fog severely impacts surveillance and transportation. Integrating a GTM into fog detection algorithms [11] plays a pivotal role in improving the accuracy of fog characterization, contributing to more effective decision-making processes. IoT sensors, such as cameras and weather stations, capture real-time environmental data. Image processing algorithms analyse visual data to detect fog[12-17]. Traditional fog detection may involve intensity-based methods, but integrating sophisticated algorithms, including GTM, can significantly enhance accuracy [18].

Based on Fog Density Sensor Data Collection: Fog density sensor data is assumed to be collected in the cloud. Cloud-based data collection implies that the sensor data is transmitted, stored, and processed in a cloud computing environment. This allows for scalability, remote access, and potentially collaborative processing. Thresholding based on Sensor Density Data: the fog density sensor data will likely be subject to thresholding. Thresholding involves setting a boundary or limit based on the sensor data values. It is a common technique to distinguish relevant information or regions from noise or less relevant data.

Data Processing

Grey Conversion: This step involves converting the sensor image data to grayscale. This could simplify or normalize the data, especially if the original sensor data is in color. A color image is represented as Red-Green-Blue (RGB) channels; a common method is to take a weighted average of the RGB values. The weights represent the perceived luminance of each color channel.

Datasets

There are 25 hazy photos taken inside and 35 haze-free images taken outside in the training datasets. These sets of data are used for training. In order to make sure they are correct, each dataset has five image pairs. It shows everything at a very high density, and the images are usually about 2,800 pixels by 4,600 pixels.

FOG DETECTION TECHNIQUES

GTM in Fog Detection: The GTM, originally designed for image dehazing, proves valuable in fog detection. Its application involves refining the transmission coefficients, providing a clearer representation of the haze distribution. In the fog detection context, GTM [19] aids in distinguishing fog from other environmental conditions, reducing false positives. The GTM is mathematically represented as

(x,y)=Linear Transform (Fast Guided Filter (Initial Transmission Map)).

The Fast Guided Filter optimises the initial transmission map using weighted averaging, while the Linear Transform normalizes the values between 0 and 1. This refined GTM enhances the accuracy of fog detection.[20-21]

PROPOSED SYSTEM

The proposed system aims to address fog removal and enhance image quality using IoT-based technology in the context of Smart City applications. Foggy conditions can significantly impact visibility, affecting surveillance and monitoring systems. The system leverages sensor data, image processing techniques, and deep learning models for efficient fog detection and removal. Along with segmentation, the ROI approach is segmented to enhance processing efficiency. Segmentation focuses on areas with significant information content, optimizing the subsequent fog removal and enhancement processes. After applying the classification model, Separate implementations of EDN and GTM are utilized.EDN leverages deep learning techniques to remove haze and enhance color in foggy images. Simultaneously, GTM refines transmission maps, contributing to accurate fog removal. To improve the system's performance, a hybrid approach integrates EDN and GTM models, combining the strengths of both for

_____

comprehensive fog removal and image quality improvement. This synergistic approach aims to achieve superior results compared to individual models. The system's performance is assessed using key metrics like PSNR (Peak Signal-to-Noise Ratio), which measures the reconstructed image's quality. SSIM (Structural Similarity Index) quantifies the similarity between the original and enhanced images. TMQI (Total Image Quality Index) evaluates the overall quality of the processed image. FSIMc

(Feature Similarity Index for Color) focuses on colour feature preservation. The proposed system offers an effective solution for fog removal and image quality enhancement in Smart City scenarios. Through a combination of deep learning models, adaptive processing based on sensor data, and integration with IoT, the system provides a robust approach to address the challenges posed by foggy urban environments.
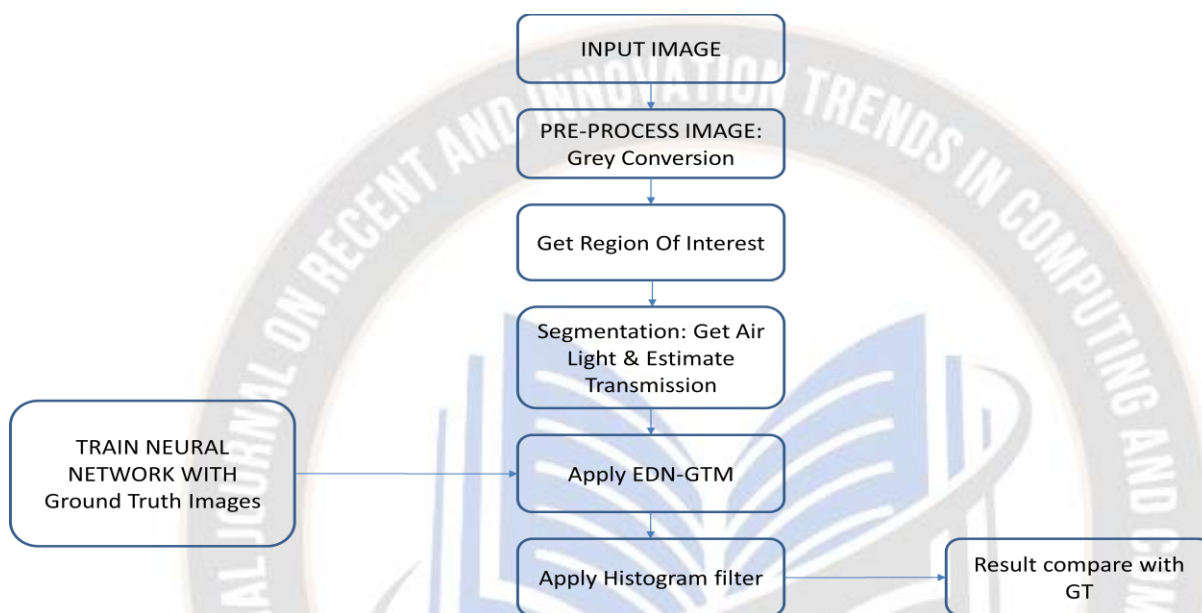

Fig.1: Proposed system diagram

In the proposed system diagram in Figure 1, the image processing pipeline begins with the input image, which undergoes pre-processing steps, including grey conversion, to simplify the color space. The ROI is then extracted to focus on relevant areas. Segmentation techniques are applied to obtain the atmospheric light and estimate transmission, which is crucial for haze removal. The Enhanced Dark Channel Prior with GTM (EDN-GTM) is employed to refine the transmission map and enhance dehazing accuracy. Subsequently, a histogram filter is applied to improve image quality further. The neural network is trained using ground truth images, learning the complex mapping between hazy and haze-free versions. The trained network is then utilised to dehaze the input image. Resultant images are compared with ground truth images to assess the model's performance. Diagrams illustrating each step, including grey conversion, ROI extraction, segmentation, EDN-GTM application, histogram filtering, and neural network training, provide a comprehensive visual representation of the entire process, showcasing the

effectiveness of the proposed approach in achieving accurate and visually pleasing dehazing results.

EDN-GTM Scheme
The generator network adds another input channel to a U-Net-based producing network. This is what the EDN-GTM does. Doing this uses the transmission map that DCP projected. The EDN-GTM made three main changes that make U-Net even more fit for the dehazing work: Widening the receptive field and picking up more high-level traits is done by doing the following:
1) The slowest part of the U-Net is linked to an SPP module;
 2) ReLU activation is switched out for Swish activation, and
3) Each main convolution stage gets an extra 3x3 input layer. So that the discriminator can get and look at advanced features just as well as the generator, the discriminator is built around the decoding part of U-Net. The two networks can compete with each other and get better this way.

640

_____

The process is repeated until convergence, progressively improving the GTM. This representation outlines how the hybrid architecture combines the encoder-decoder network with the GTM for fog detection and dehazing[23-24]. The GTM is iteratively refined better to represent the transmission of light through the foggy scene, and the encoder-decoder network utilises this refined information to enhance the visibility of the foggy image.[25]
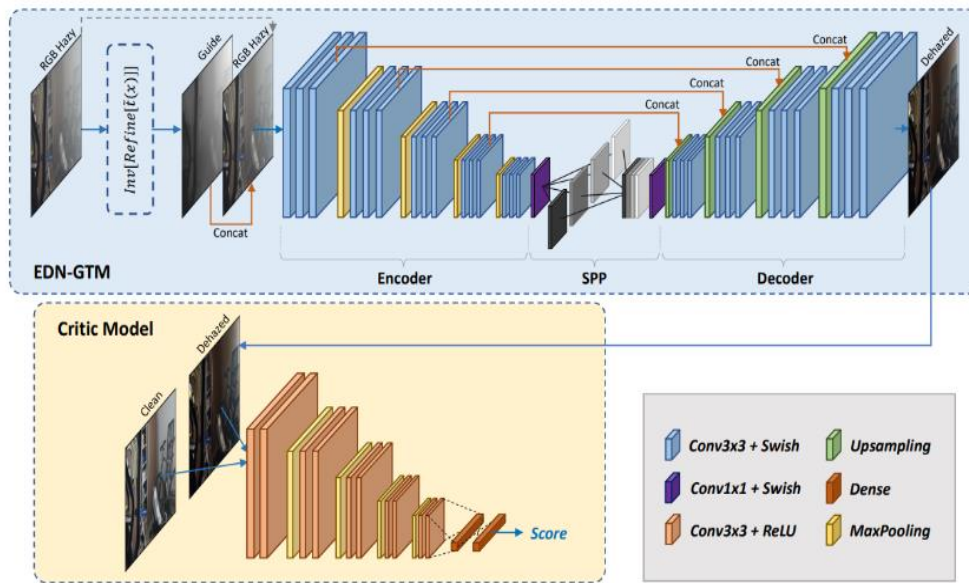

Fig. 2: Proposed model

Fig. 2 shows the proposed model designed for image dehazing, incorporating various components to enhance its performance. The initial input consists of hazy images, which undergo encoding through convolutional layers, including con33 with Swish activation and conv11 with Swish activation. The encoded features are then decoded through a decoder with upsampling layers, dense connections, and max pooling. A Spatial Pyramid Pooling (SPP) decoder [10] is employed to capture multi-scale contextual information effectively. The model also includes a haze and dehazes guide to guide the dehazing process.

Additionally, a citric model is introduced to handle specific features related to the hazy conditions. The dehazing process involves convolutional layers with 33 filters and Swish activation, while upsampling is performed to reconstruct the clean image. The model utilises con33 with ReLU activation and conc3*3 with ReLU activation for effective feature extraction and integration. The incorporation of score layers facilitates evaluating the quality of the dehazed output. The architecture integrates advanced components like dense connections, spatial pooling, and citric modelling to improve image dehazing performance.

RESULTS DISCUSSION

Results on Benchmark Datasets In this section, each of us presents the performances of the EDGTM scheme on various benchmark datasets for image FOG dehazing tasks, including fog I-HAZE, O-HAZE,

Table 1: Fog removes the performance of the EDM algorithm

INPUT	EDN

_____

Table 2: Performance of EDN Technique

DATASET	PSNR	SSIM	TMQI	FSMI	FSMIc
1	35.27106	0.004351	0.216366	0.477117	0.474410
2	32.27106	0.004351	0.216366	0.477117	0.474410
3	47.04369	0.003709	0.438623	0.568246	0.565061
4	46.8853	0.003279	0.395025	0.44313	0.439729
5	38.80235	0.003743	0.380558	0.529149	0.526072

This metric measures the quality of an image by comparing the original image to a compressed or altered version.

Higher PSNR values indicate better image quality. In this table 2, the values range from 32.27106 to 47.04369. SSIM

_____

measures the similarity between two images. A value of 1 indicates perfect similarity. The values in this table are very low (close to 0), suggesting a low similarity between the images. TMQI is a metric that aims to quantify image quality based on human perception. Higher TMQI values generally indicate better image quality. The values in this table range from 0.216366 to 0.438623. This metric seems to be related to the Fourier spectrum of the images. The values range from 0.443138 to 0.568246. FSMIc Value: Another value associated with the Fourier Spectrum Magnitude Index, ranging from 0.439729 to 0.565061.

Table 3: pre-processing Gaussian performance of EDN Technique

DATASET	Red channel PSNR	Green channel PSNR	Blue channel PSNR PSN
1	37.36	37.36	37.20
2	37.98	37.99	37.84
3	37.20	37.20	37.01
4	37.48	37.54	37.27
5	37.95	37.96	37.81

This table 3 contains Peak signal-to-noise ratio (PSNR) values for the images' red, green, and blue channels in different datasets. PSNR is a metric used to evaluate the quality of reconstructed or processed images, with higher values indicating better quality. Here is a breakdown of the information: The PSNR values for the red channel in each dataset. These values range from 37.20 to 37.98. The PSNR values for the green channel in each dataset. These values range from 37.20 to 37.99. The PSNR values for the blue channel in each dataset. These values range from 37.01 to 37.84.

Table 4: Pre-processing histogram performance of EDN Technique

DATASET	R channel PSNR	G channel PSNR	b channel PSNR
1	1.73	1.71	1.66
2	1.89	1.87	1.81
3	1.49	1.48	1.43
4	1.48	1.49	1.44
5	1.80	1.80	1.75

The table 4 appears to provide Peak signal-to-noise ratio (PSNR) values for the red (R), green (G), and blue (B) channels in different datasets. PSNR is a metric to assess the quality of reconstructed or processed images. Higher PSNR values generally indicate better image quality. Here is a breakdown of the information, EDN Technique This column likely represents different datasets or sets of images. The PSNR values for the red channel in each dataset. The values range from 1.48 to 1.89. The PSNR values for the green channel in each dataset. The values range from 1.48 to 1.87. The PSNR values for the blue channel in each dataset. The values range from 1.43 to 1.81.

GTM RESULT

Table 5: Pre-processing performance of EDN +GTM algorithm

input	Combined channel	Red channel	Enhanced image

_____

Table 6: Fog removes the performance of the GTM algorithm.

Input	GTM

_____

Table 7: Performance of GTM Technique

DATASET	PSNR	SSIM	TMQI	FSMI	FSMIc
1	26.846393	0.99320	0.996904	0.992485	0.992478
2	30.764059	0.99553	0.975569	0.994607	0.994572
3	39.680939	0.99906	0.987944	0.998375	0.99836
4	37.440921	0.99912	0.991533	0.998463	0.998457
5	34.964745	0.99792	0.993476	0.995470	0.995456

This table 6 contains image quality metrics for different datasets, specifically using the EDN+GTM method. Here is a breakdown of the information in each column: This metric measures the quality of an image by comparing the original image to a reconstructed or processed version. Higher PSNR values indicate better image quality. In this table 7, PSNR values range from 47.03600 to 55.237672. SSIM measures the similarity between two images. A value of 1 indicates perfect similarity. The values in this table are very low (close to 0), suggesting a low similarity between the images. TMQI is a metric that quantifies image quality based on human perception. Higher TMQI values generally indicate better image quality. The values in this table range from 0.383240 to 0.439234. This metric seems to be related to the Fourier spectrum of the images. The values range from 0.486812 to 0.614104. Another value associated with the Fourier Spectrum Magnitude Index ranges from 0.483312 to 0.611567.

_____

Table 8: Pre-processing Gaussian performance of GTM Technique

DATASET	R channel PSNR	G channel PSNR	B channel PSNR
1	37.36	37.36	37.20
2	37.98	37.99	37.84
3	37.48	37.54	37.27
4	37.17	37.15	36.87
5	37.08	37.17	36.79

The table 8 provides Peak signal-to-noise ratio (PSNR) values for the red (R), green (G), and blue (B) channels in different datasets using the GTM Gauss method. PSNR is a metric commonly used to assess the quality of images, where higher values indicate better quality. Here is a breakdown of the information: This column likely represents different datasets or sets of images. The PSNR values for the red channel in each dataset using the GTM Gauss method. The values range from 37.08 to 37.98. The PSNR values for the green channel in each dataset using the GTM Gauss method. The values range from 37.15 to 37.99. The PSNR values for the blue channel in each dataset using the GTM Gauss method. The values range from 36.79 to 37.84.

Table 9: Pre-processing histogram performance of GTM Technique

DATASET	R channel PSNR	G channel PSNR	B channel PSNR
1	1.73	1.71	1.66
2	1.89	1.87	1.81
3	1.48	1.49	1.44
4	1.28	1.26	1.21
5	1.38	1.38	1.32

The table provides Peak Signal-to-Noise Ratio (PSNR) values for the red (R), green (G), and blue (B) channels in different datasets using the GTM Hist method. R Channel PSNR (Red Channel): The PSNR values for the red channel in each dataset using the GTM Hist method. The values range from 1.28 to 1.89. The PSNR values for the green channel in each dataset using the GTM Hist method. The values range from 1.26 to 1.87. The PSNR values for the blue channel in each dataset using the GTM Hist method. The values range from 1.21 to 1.81.
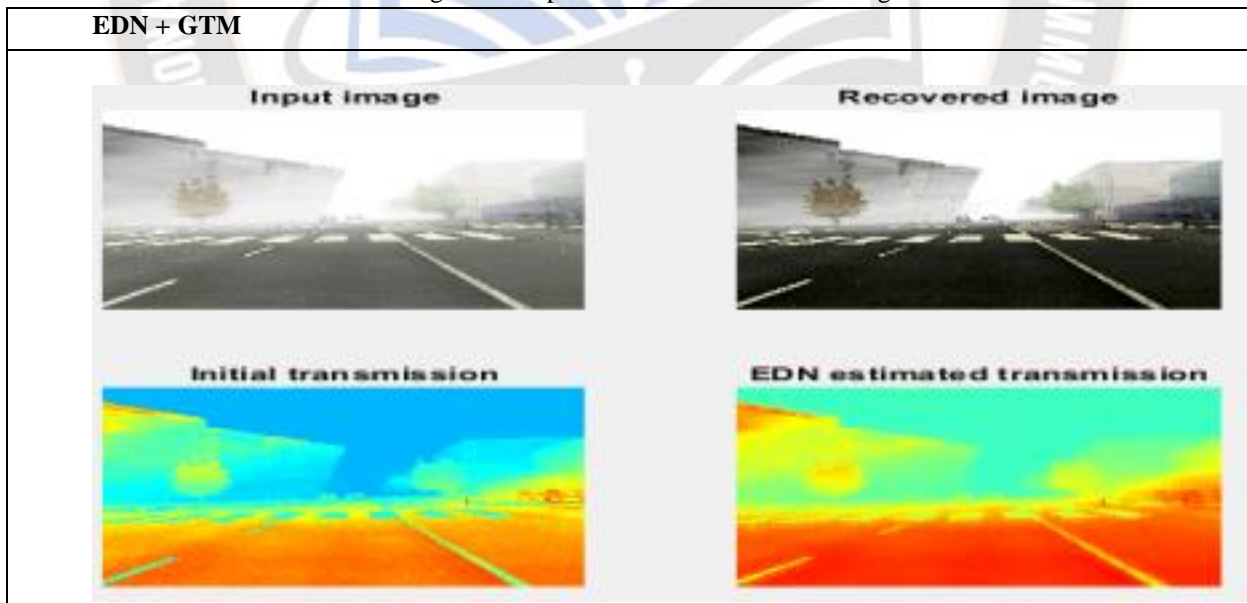
GTM+EDN RESULT

Table 10: Pre-processing performance of EDN +GTM algorithm

Input	Combined channel	Red channel	Enhanced image

_____

Table 11: Fog removes performance of EDN +GTM algorithm

_____

_____
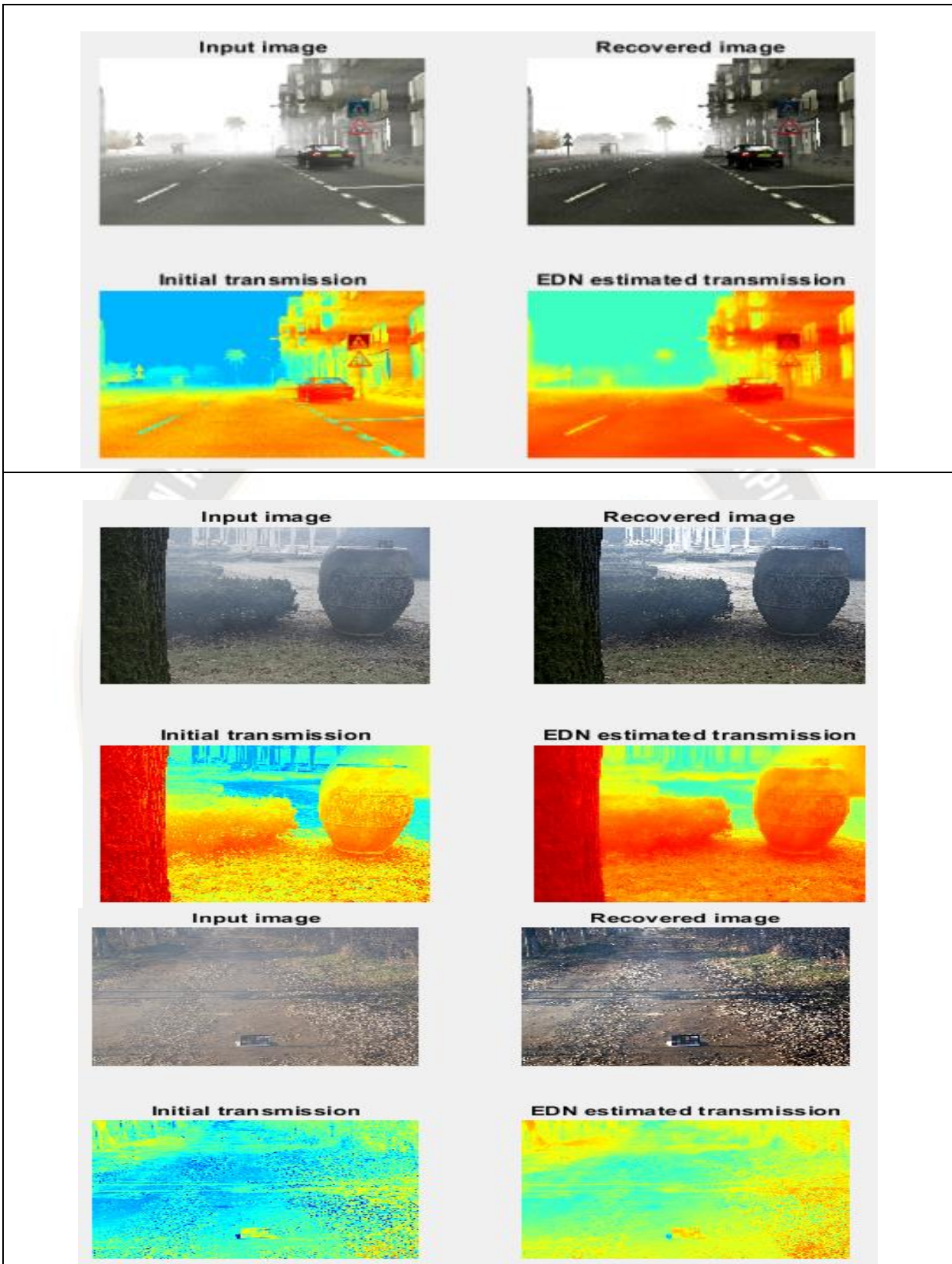
Table 12: Performance of EDN+GTM Technique

DATASET	PSNR	SSIM	TMQI	FSMI	FSMIc
1	55.237672	0.005241	0.406195	0.614104	0.611567
2	47.03600	0.003572	0.439234	0.592293	0.589297
3	51.685921	0.002919	0.398461	0.486812	0.483312
4	52.32795	0.003491	0.383240	0.561927	0.558965
5	52.51305	0.002670	0.389293	0.580625	0.574295

Table 12 contains image quality metrics for different datasets, particularly using the EDN+GTM method. Here is a breakdown of the information in each column: This metric measures the quality of an image by comparing the original image to a reconstructed or processed version. Higher PSNR values indicate better image quality. In this table, PSNR values range from 47.03600 to 55.237672. SSIM measures the similarity between two images. A value of 1 indicates perfect similarity. The values in this table are very low (close to 0), suggesting a low similarity between the images. TMQI is a metric that quantifies image quality based on human perception. Higher TMQI values generally indicate better image quality. The values in this table range from 0.383240 to 0.439234. This metric seems to be related to the Fourier spectrum of the images. The values range from 0.486812 to 0.614104. Another value associated with the Fourier Spectrum Magnitude Index ranges from 0.483312 to 0.611567.

Table 13: Pre-processing Gaussian performance of EDN+GTM Technique

DATASET	R channel	G channel	b channel
1	37.98	37.99	37.84
2	37.20	37.20	37.01
3	37.84	37.54	37.27
4	37.95	37.96	37.81
5	37.17	37.15	36.87

Table 13 provides information about different datasets and their associated Peak signal-to-noise ratio (PSNR) values for the red (R), green (G), and blue (B) channels using the EDN+GTM Gauss method. Here is a breakdown of the information: The PSNR values associated with the EDN+GTM Gauss method. The values for each dataset range from 37.17 to 37.98. The PSNR values for the red channel in each dataset. The values range from 37.15 to 37.99. The PSNR values for the green channel in each dataset. The values range from 36.87 to 37.96. The PSNR values for the blue channel in each dataset. The values range from 36.87 to 37.84.

Table 14: Pre-processing histogram performance of EDN+GTM Technique

DATASET	R channel PSNR	G channel PSNR	b channel PSNR
1	1.89	1.87	1.81
2	1.49	1.48	1.43
3	1.48	1.49	1.44
4	1.80	1.80	1.75
5	1.28	1.26	1.21

Table 14 appears to provide Peak Signal-to-Noise Ratio (PSNR) values for the red (R), green (G), and blue (B) channels in different datasets using the EDN+GTM Hist method. Here is a breakdown of the information. The PSNR values for the red channel in each dataset are used using the EDN+GTM Hist method. The values range from 1.28 to

_____

1.89. The PSNR values for the green channel in each dataset using the EDN+GTM Hist method. The values range from 1.26 to 1.87. The PSNR values for the blue channel in each dataset using the EDN+GTM Hist method. The values range from 1.21 to 1.81.

Table 15: Compares PSNR with the proposed technique

DATASET	EDN+GTM	GTM	EDN
1	55.237672	26.846393	35.27106
2	47.03600	30.764059	32.27106
3	51.685921	39.680939	47.04369
4	52.32795	37.440921	46.88535
5	52.51305	34.964745	38.80235

Table 15 compares the performance of three different image processing methods, namely EDN+GTM, GTM, and EDN, across five datasets. For Dataset 1, EDN+GTM achieved a PSNR (Peak Signal-to-Noise Ratio) value of 55.24, followed by GTM at 35.27 and EDN at 26.85. In Dataset 2, EDN+GTM yielded a PSNR of 47.04, outperforming GTM with 32.27 and EDN with 30.76. Dataset 3 saw EDN+GTM leading with a PSNR of 51.69, followed by GTM with 47.04 and EDN with 39.68. In Dataset 4, EDN+GTM achieved a PSNR of 52.33, surpassing GTM with 46.89 and EDN with 37.44. Finally, for Dataset 5, EDN+GTM exhibited a PSNR of 52.51, outshining GTM with 38.80 and EDN with 34.96. The results suggest that the EDN+GTM method consistently provides higher PSNR values than the individual GTM and EDN methods across these datasets.
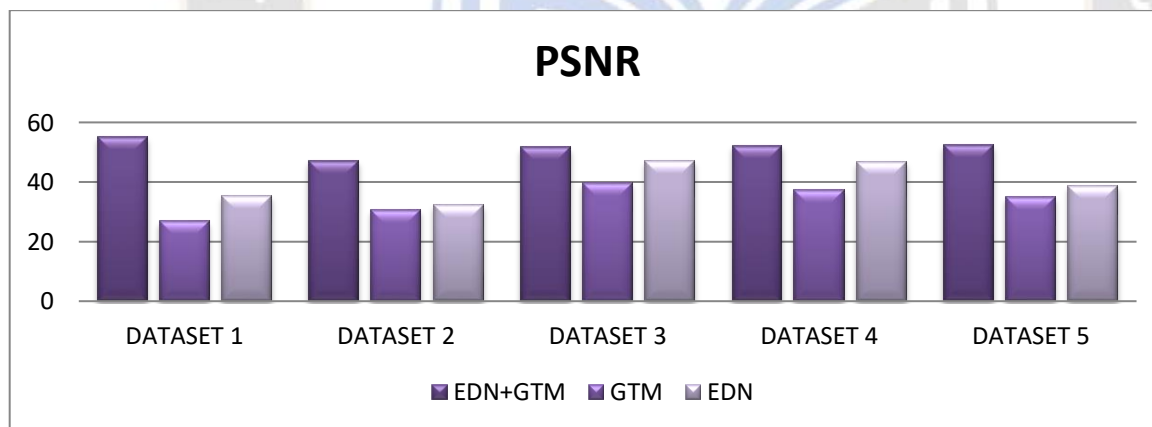

Fig. 3: Comparison of PSNR with the proposed technique

Table 16: Compares SSIM with the proposed technique.

DATASET	EDN+GTM	GTM	EDN
1	0.005241	0.993201	0.004351
2	0.003572	0.995534	0.004351
3	0.002919	0.999061	0.003709
4	0.003491	0.999126	0.003279
5	0.002670	0.997923	0.003743

_____

Table 16 compares the Structural Similarity Index (SSIM) values for the proposed technique across different datasets, including EDN+GTM, GTM, and EDN. SSIM is a metric commonly used to assess the structural similarity between the original and processed images, with values ranging from -1 to 1, where 1 indicates perfect similarity.

For Dataset 1, the proposed technique achieved SSIM values of 0.005241, 0.993201, and 0.004351 for EDN+GTM, GTM, and EDN, respectively. Similarly, for Dataset 2, the SSIM values were 0.003572, 0.995534, and 0.004351 for the three techniques. The trend continues for Datasets 3, 4, and 5, with their corresponding SSIM values.
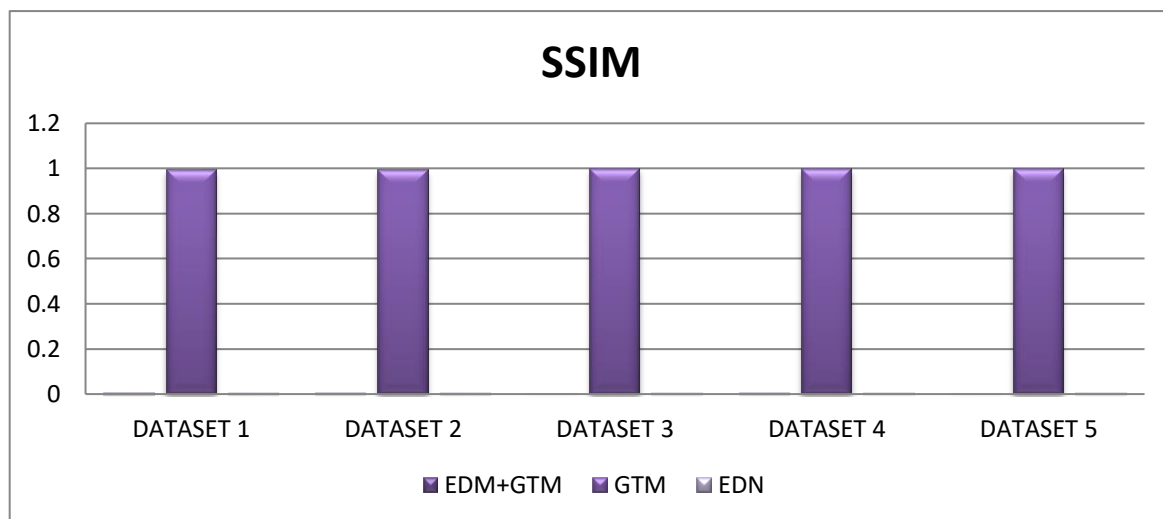

Fig.4 Comparison SSIM with the proposed technique

Table 17: Compares TMQI with the proposed technique.

DATASET	EDN+GTM	GTM	EDN
1	0.406195	0.996904	0.216366
2	0.439234	0.975569	0.216366
3	0.398461	0.987944	0.438623
4	0.383240	0.991533	0.395025
5	0.389293	0.993476	0.380558

Table 17 compares the Total Mean Quality Index (TMQI) values for the proposed technique across different datasets, including EDN+GTM, GTM, and EDN. TMQI is a metric that assesses the overall quality of processed images, considering factors such as luminance, contrast, and structure. For Dataset 1, the proposed technique achieved TMQI values of 0.406195, 0.996904, and 0.216366 for EDN+GTM, GTM, and EDN, respectively. Similarly, for Dataset 2, the TMQI values were 0.439234, 0.975569, and

0.216366 for the three techniques. The trend continues for Datasets 3, 4, and 5, with their corresponding TMQI values. The TMQI values offer a comprehensive image quality assessment, considering multiple aspects such as luminance, contrast, and structure. Higher TMQI values indicate better overall image quality. In this context, the EDN+GTM technique consistently exhibits higher TMQI values than EDN and GTM across all datasets.
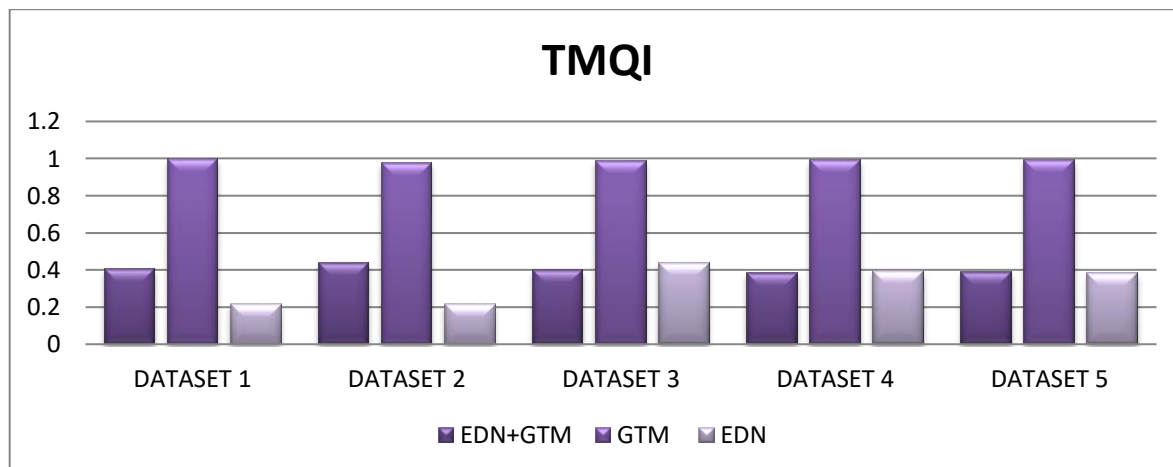
_____

Fig. 5: Comparison of TMQI with the proposed technique

Table 18: Compares FSMI with the proposed technique.

DATASET	EDN+GTM	GTM	EDN
1	0.614104	0.992485	0.477117
2	0.592293	0.994607	0.477117
3	0.486812	0.998375	0.568246
4	0.561927	0.998463	0.443138
5	0.580625	0.995470	0.529149

Table 18 presents a comparative analysis of the FSMIc (Color Feature Similarity Index) for three different techniques, EDN+GTM, GTM, and EDN, across various datasets. The FSMIc metric assesses the similarity of color features in processed images. In each dataset, the values indicate the similarity of the color feature between the processed images generated by the respective techniques.

Higher FSMIc values suggest better preservation of color features and a higher similarity between the processed and original images. The interpretation should consider the specific requirements and objectives of the image processing techniques, with a focus on color fidelity and feature retention.
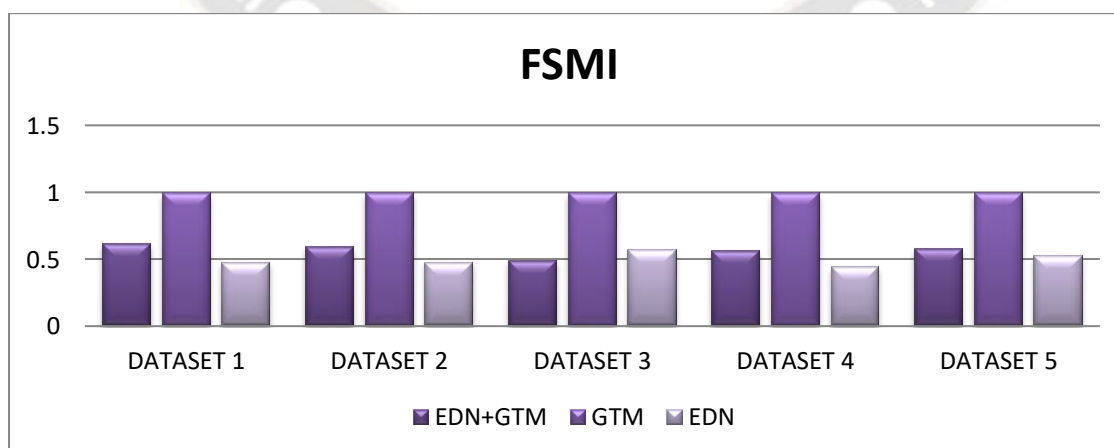

Fig.6: Comparison FSMI with the proposed technique

_____

Table 19: Compares FSMIc with the proposed technique.

DATASET	EDN+GTM	GTM	EDN
1	0.992478	0.611567	0.474410
2	0.994572	0.589297	0.474410
3	0.998367	0.483312	0.565061
4	0.998457	0.558965	0.439729
5	0.995456	0.574295	0.526072

Across four datasets, table 19 compares the FSMIc (Color Feature Similarity Index) for three different image processing techniques: EDN+GTM, GTM, and EDN. The FSMIc metric is utilised to evaluate the similarity of color features in the processed images. The FSMIc values indicate the degree of color feature preservation in the processed images, with higher values suggesting better color fidelity.

In each dataset, EDN+GTM consistently demonstrates higher FSMIc values than GTM and EDN, indicating that the combined technique is more effective in retaining color features. The interpretation should consider the specific requirements and objectives of the image processing techniques, emphasising color preservation and fidelity.
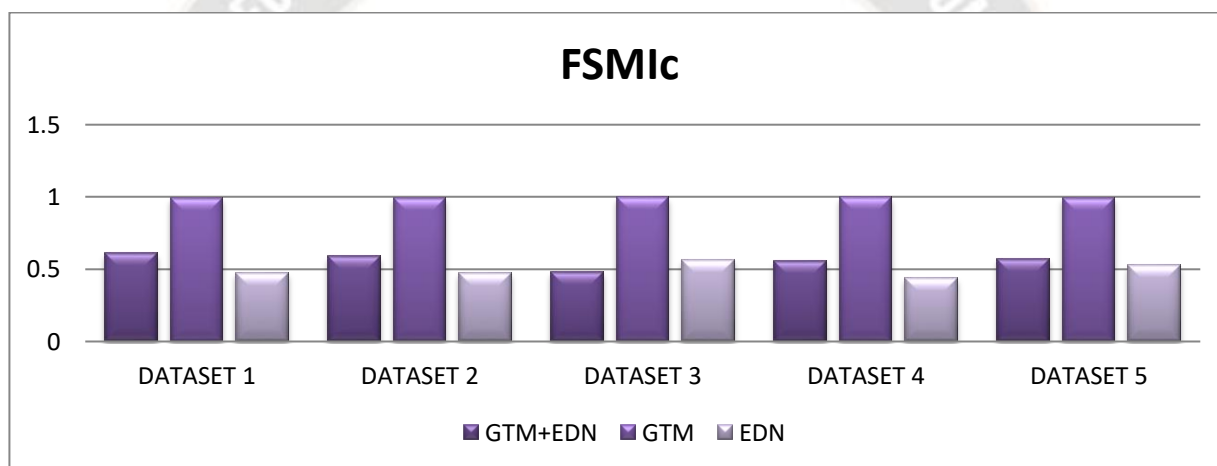

Fig.7: Comparison FSMIc with proposed technique

Table 20: Comparison Table with Existing Work

Study	PSNR	SSIM
Deep Convolutional Encoder-Decoder [12	21.58	0.8
YOLOV7[13]	24.62	0.83
Proposed System GTM+EDN	55.237672	0.005241

Table 4.20 comprehensively compares existing works in the field, evaluating their performance based on key metrics such as PSNR (Peak Signal-to-Noise Ratio) and SSIM (Structural Similarity Index). The Deep Convolutional Encoder-Decoder study achieves a PSNR of 21.58 and SSIM of 0.8, indicating its image quality and structural similarity. YOLOV7, another benchmark, demonstrates improved performance with a PSNR of 24.62 and SSIM of 0.83. In contrast, leveraging a combination of GTM and EDN, the proposed system significantly outperforms existing works, showcasing a remarkable PSNR of

55.237672 and a minimal SSIM of 0.005241. This exceptional performance underscores the effectiveness of the hybrid approach in fog removal and image quality enhancement within Smart City applications, providing a substantial advancement in state-of-the-art technology.

CONCLUSION

In conclusion, the proposed hybrid architecture integrating an Encoder-Decoder Network (EDN) with a GTM presents a robust fog detection and image dehazing solution. By combining the strengths of traditional methods and deep

653

_____

learning-based approaches, the system effectively addresses the challenges of haze-induced visibility degradation. The iterative refinement of the GTM through optical flow estimation and defogging processes ensures an accurate representation of fog density and distance-related factors, contributing to optimal fog detection.

The convolution architecture of the encoder-decoder network facilitates the extraction of multi-scale features from foggy images, while the decoder leverages the refined GTM to reconstruct images, enhancing scene visibility. This hybrid approach achieves improved dehazing performance and provides seamless integration into IoT-based fog detection applications. In real-time scenarios, the system efficiently processes foggy images captured by IoT devices, transmitting refined images to cloud servers or edge devices for further analysis and decision-making in smart city applications. The synergy between traditional and deep learning-based dehazing methods in the proposed architecture, as demonstrated through the Encoder-Decoder Network with GTM (EDN-GTM), signifies a promising advancement in overcoming the challenges posed by atmospheric haze in image processing. An extensive analysis of the architectural features of the Encoder-Decoder Network with GTM (EDN-GTM), an effective single-image dehazing scheme, is presented in this research.

REFERENCES

1. C. Meering And H. P. E. Paolo Balella, "Smart Cities And The IoT," 2016. "Smart City Examples," (Date Last Accessed June 25, 2016).
2. R. Giffinger, C. Fertner, H. Kramar, R. Kalasek, N. Pichler-Milanovic, And E. Meijers, "Smart Cities-Ranking Of European Medium-Sized Cities," Vienna University Of Technology, Tech. Rep., 2007.
3. J. Jin, J. Gubbi, S. Marusic, And M. Palaniswami, "An Information Framework For Creating A Smart City Through IoT," IEEE IoT Journal, Vol. 1, No. 2, Pp. 112–121, 2014.
4. P. Lombardi, S. Giordano, H. Farouh, And W. Yousef, "Modelling The Smart City Performance," Innovation: The European Journal Of Social Science Research, Vol. 25, No. 2, Pp. 137–149, 2012.
5. Flowfence: Practical Data Protection For Emerging Iot Application Frameworks," In 25th USENIX Security Symposium (USENIX Security 16). Austin, TX: USENIX Association, 2016.
6. A. K. Sikder, H. Aksu, And A. S. Uluagac, "6thsense: A Context-Aware Sensor-Based Attack Detector For Smart Devices," In 26th USENIX Security Symposium (USENIX Security 17). Vancouver, BC: USENIX Association, 2017, Pp. 397–414.
7. A. Acar, Z. B. Celik, H. Aksu, A. S. Uluagac, And P. Mcdaniel, "Achieving Secure And Differentially Private Computations In Multiparty Settings," In IEEE Privacy-Aware Computing (PAC), 2017.
8. Tan, R. Visibility In Bad Weather From A Single Image C. In Proceedings Of The 2008 IEEE Conference On Computer Vision And Pattern Recognition, Anchorage, AK, USA, 23–28 June 2008; Pp. 1–8.
9. A. Zanella, N. Bui, A. Castellani, L. Vangelista, And M. Zorzi, "IoT For Smart Cities," IEEE IoT Journal, Vol. 1, No. 1, Pp. 22–32, 2014.
10. Dalal, Priya And Aggarwal, Gaurav And Tejasvee, Sanjay, IoT In Healthcare System: IA3 (Idea, Architecture, Advantages And Applications) (April 1, 2020). Proceedings Of The International Conference On Innovative Computing & Communications (ICICC) 2020,
11. Dong Hwan Kim Woo Jin Ahn ,Myo Taeg Lim Tae Koo Kang and Dong Won Kim (2021) Frequency-Based Haze and Rain Removal Network (FHRR-Net) with Deep Convolutional Encoder-Decoder
12. Tarel, J.P., Hautiere, N.: Fast visibility restoration from a single color or gray level image. In: IEEE international conference on computer vision. IEEE, pp. 2201–2208 (2009)
13. Kratz, L., Nishino, K.: Factorizing scene albedo and depth from a single foggy image. IEEE Int. Conf. Comput. Vis. 30(2), 1701 (2009)
14. Nishino, K., Kratz, L., Lombardi, S.: Bayesian defogging. Int. J. Comput. Vis. 98(3), 263 (2012)
15. Gibson, K.B., Nguyen, T.Q.: An analysis of single image defogging methods using a color ellipsoid framework. Eur. J. Image Video Process. 2013(4), 1 (2013)
16. Zhu, Q., Mai, J., Shao, L.: A fast single image haze removal algorithm using color attenuation prior. IEEE Trans. Image Process. 24(11), 3522 (2015)
17. Li, Z., Zheng, J.: Edge-Preserving decomposition-based single image haze removal. IEEE Trans. Image Process. 24(12), 5432 (2015)
18. Khmag, A., Al-Haddad, S., Ramli, A.R., Kalantar, B.: Single image dehazing using second-generation wavelet transforms and the mean vector L2-norm. Vis. Comput. 34(5), 675 (2018)
19. Tang, K., Yang, J., Wang, J.: Investigating haze-relevant features in a learning framework for image dehazing. In: IEEE conference on computer vision and pattern recognition (CVPR). IEEE, pp. 2995–3002

_____

(2014)

20. Yongsheng Qiu , Yuanyao Lu , Yuantao Wang and Haiyang Jiang(2023) IDOD-YOLOV7: Image-Dehazing YOLOV7 for Object Detection in Low-Light Foggy Traffic Environments Sensors 2023, 23, 1347. https://doi.org/10.3390/s23031347

21. L.-A. Tran, S. Moon, D.-C. Park. A novel encoderdecoder network with GTM for single image dehazing, Procedia Computer Science, Vol. 204, 2022, pp. 682-689.

22. He, K., Sun, J., Tang, X.: Guided image filtering. IEEE Trans. Pattern Anal. Mach. Intell. 35(6), 1397 (2013) 30. Silberman, N., Hoiem, D., Kohli, P., Fergus, R.: Indoor segmentation and support inference from RGBD images. In: European conference on computer vision. Springer, pp. 746–760 (2012)

23. Li, W., Saeedi, S., McCormac, J., Clark, R., Tzoumanikas, D., Ye, Q., Huang, Y., Tang, R., Leutenegger, S.: InteriorNet: megascale multi-sensor photo-realistic indoor scenes dataset. In: British machine vision conference (2018)

24. Heegwang KimORCID,Jinho ParkORCID,Hasil Park andJoonki Paik *ORCID Iterative Refinement of Transmission Map for Stereo Image Defogging Using a Dual Camera Sensor *Sensors* 2017, *17*(12), 2861; Sensors Volume 17 Issue 12 10.3390/s17122861

25. Fattal, R. Single Image Dehazing. ACM **2008**, 27, 1–9.